

Probing Two-Photon Properties of Molecules: Large Non-Condon Effects Dominate the Resonance Hyper-Raman Scattering of Rhodamine 6G

Chris B. Milojevich,[†] Daniel W. Silverstein,[‡] Lasse Jensen,^{*,†} and Jon P. Camden^{*,†}

[†]Department of Chemistry, University of Tennessee, Knoxville, Tennessee 37996-1600, United States

[‡]Department of Chemistry, Pennsylvania State University, University Park, Pennsylvania 16802, United States

 Supporting Information

ABSTRACT: Experimentally measured resonance hyper-Raman (RHR) spectra spanning the $S_1 \leftarrow S_0$, $S_2 \leftarrow S_0$, and $S_3 \leftarrow S_0$ transitions in rhodamine 6G (R6G) have been recorded. These spectra are compared to the results of first-principles calculations of the RHR intensity that include both Franck–Condon (A-term) and non-Condon (B-term) scattering effects. Good agreement between the experimental and theoretical results is observed, demonstrating that first-principles calculations of hyper-Raman intensities are now possible for large molecules such as R6G. Such agreement indicates that RHR spectroscopy will now be a routine aid for probing multiphoton processes. This work further shows that optimization of molecular properties to enhance either A- or B-term scattering might yield molecules with significantly enhanced two-photon properties.

There is significant interest in utilizing multiphoton processes for applications in all-optical switching, energy-up conversion, and biological imaging.^{1–4} For example, two-photon transitions can be used in optical-power-limiting materials, photodynamic therapy, optical data storage, two-photon fluorescence microscopy, and two-photon photopolymerization for three-dimensional lithographic microfabrication.^{2–7} Two-photon techniques also provide a method to probe “dark” electronic states, i.e., those that are either forbidden or only weakly allowed via one-photon excitation.⁸

Hyper-Raman scattering⁹ is a type of nonlinear light scattering in which a photon at $\omega = 2\omega_0 - \omega_v$ is incoherently scattered, where ω_0 is the laser frequency and ω_v is a vibrational frequency characteristic of the material. Resonance hyper-Raman (RHR) scattering provides detailed information about the geometry of two-photon-accessible excited states. For weakly allowed one- or two-photon transitions, RHR scattering provides additional information about non-Condon effects, i.e., the nuclear dependence of the one- or two-photon transition moments. The framework provided by the vibronic theory of RHR scattering¹⁰ interprets the observed scattering intensities in terms of vibronic coupling terms, Franck–Condon factors, and one- and two-photon dipole moments and their nuclear dependence. This rich set of information, however, is not easily interpreted because of the complex interplay of the various excited states and their topology.

In this communication, we report a detailed comparison of experimentally measured and theoretically calculated RHR intensities spanning the $S_1 \leftarrow S_0$, $S_2 \leftarrow S_0$, and $S_3 \leftarrow S_0$ transitions in rhodamine 6G (R6G). This comparison has allowed us to identify and quantify the various contributions to the RHR intensities and demonstrates that reliable calculations of RHR spectra including both Franck–Condon and non-Condon effects are now possible for large molecules such as R6G. Furthermore, we have found that the hyper-Raman scattering of R6G is dominated by non-Condon effects and that interference between the two lowest electronic states plays an essential role, even though they are separated by more than 100 nm (~ 0.4 eV).

RHR and surface-enhanced hyper-Raman scattering (SEHRS)^{11–14} spectra were recorded for excitation wavelengths spanning the two-photon absorption spectrum of R6G. For some of the wavelengths in this region, the large two-photon fluorescence of R6G hinders the collection of RHR spectra. The fluorescence quenching provided by Ag nanoparticles, however, removes this limitation. The concentration of R6G was 10^{-7} M for the SEHRS studies and 10^{-3} M for the aqueous-solution-phase RHR measurements. The laser bandwidth was narrowed in comparison to our previous studies⁸ by increasing the pulse length to ~ 6 ps.

Figure 1 displays the RHR (Figure 1a) and SEHRS spectra (Figure 1b) of R6G at $\lambda = 825$ nm. While there are minor differences between the RHR and SEHRS spectra, the good agreement suggests that surface effects are a minor perturbation on the spectra. Figure 1 also compares the experimental spectra with first-principles simulations using a time-dependent formalism for describing the RHR scattering. The molecular properties needed for simulating the hyper-Raman scattering were obtained using time-dependent density functional theory (TDDFT) at the B3LYP/6-311G* level. Details of the simulations are provided in the Supporting Information (SI). Our simulations included the three lowest excited states (S_1 , S_2 , and S_3) and explored Franck–Condon (A-term) and non-Condon (B-term) scattering effects.

Good agreement between the theory and experiment was obtained when both A- and B-term scattering was included (Figure 1a–c). The spectrum calculated using only Franck–Condon effects (Figure 1d) did not agree with experiment. A further comparison of the experimental and theoretical spectra for wavelengths spanning the S_1 , S_2 , and S_3 transitions is displayed in Figure 2.

Received: June 21, 2011

Published: August 18, 2011

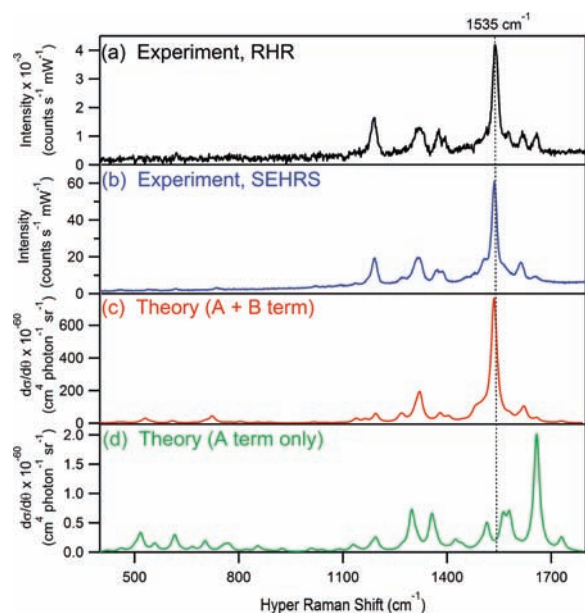


Figure 1. Comparison of experimentally measured and theoretically calculated RHR spectra of R6G at $\lambda = 825$ nm. (a) RHR spectrum of 10^{-3} M R6G in water. (b) SEHRS spectrum of R6G on aggregated silver colloids. (c) TDDFT calculation of the RHR spectrum including both Franck–Condon (A-term) and non-Condon (B-term) scattering. (d) Spectrum calculated including only A-term scattering. The spectra were measured and calculated on resonance with the two-photon $S_2 \leftarrow S_0$ transition.

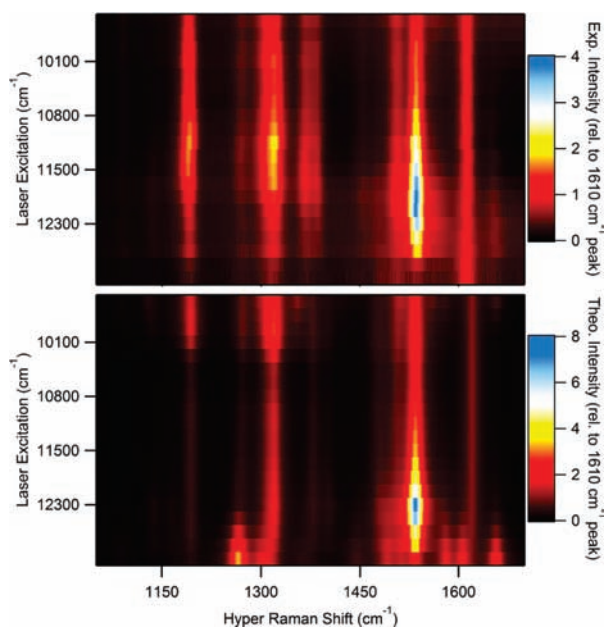


Figure 2. Comparison of (top) experimentally measured and (bottom) theoretically calculated hyper-Raman spectra of R6G for excitation wavelengths between 750 and 1050 nm.

To the best of our knowledge, this represents the first first-principles calculation of RHR intensities that includes non-Condon effects for a molecule as large as R6G.

We now interpret these effects with reference to the one- and two-photon absorption spectrum of R6G shown in Figure 3. In a

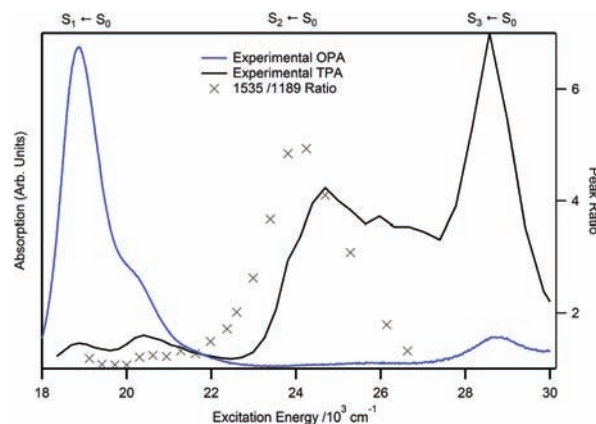


Figure 3. Comparison of the experimentally measured one-photon (blue) and two-photon (black; ref 15) absorption spectra of R6G. The ratio of the 1535 and 1189 cm^{-1} peaks (\times) is reproduced from ref 8.

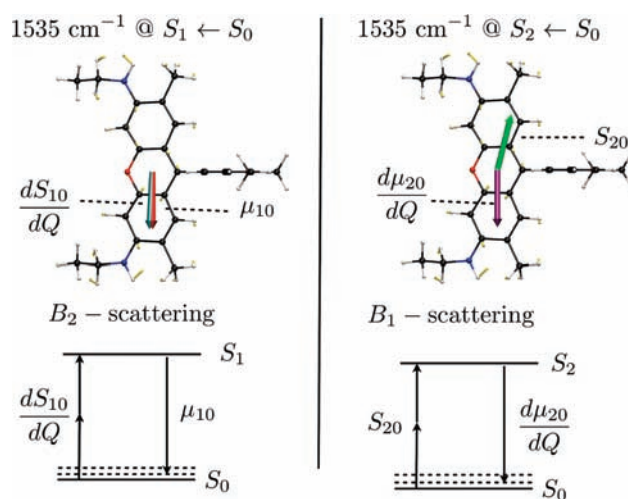


Figure 4. Non-Condon effects in R6G. The hyper-Raman scattering resonant with the S_1 state is dominated by B_2 scattering, where the non-Condon effects arise from the nuclear dependence of the two-photon transition moment. For the S_2 state, the hyper-Raman scattering is dominated by B_1 scattering, where the non-Condon effects arise from the one-photon transition moment. Depicted for each electronic state are the normal mode of the 1535 cm^{-1} vibration and the corresponding one- and two-photon transition moments.

previous study,⁸ we found that the dominant 1535 cm^{-1} band is correlated with the $S_2 \leftarrow S_0$ transition. The $S_2 \leftarrow S_0$ transition is two-photon-allowed, but only *weakly* one-photon-allowed; therefore, the non-Condon effects arise from the nuclear dependence of the transition dipole moment (the B_1 term). In contrast, the $S_1 \leftarrow S_0$ transition is strongly one-photon-allowed but only weakly two-photon-allowed; therefore, on resonance with S_1 , the non-Condon effects arise from the nuclear dependence of the two-photon transition moments (the B_2 term). Figure 4 compares the B_2 and B_1 terms for the two states and displays the normal mode associated with the strongest vibrational band (1535 cm^{-1}) observed on resonance with S_2 . From these data, we must conclude that the hyper-Raman spectrum of R6G is characterized by significant non-Condon effects for both the S_1 and S_2 states.

Non-Condon scattering is typically weak because either the two-photon or one-photon electronic transition is forbidden (or nearly so). Our simulations show, however, that R6G has a large differential hyper-Raman cross section of $7.6 \times 10^{-58} \text{ cm}^4 \text{ s photon}^{-1} \text{ sr}^{-1}$ on resonance with the S_2 state. At this wavelength, the contribution from the B term is ~ 300 times stronger than the contribution from the A term. For comparison, the hyper-Raman differential cross section of *p*-nitroaniline (PNA), a prototypical push–pull molecule with a significant hyperpolarizability, is only $4.1 \times 10^{-58} \text{ cm}^4 \text{ s photon}^{-1} \text{ sr}^{-1}$ on resonance with a state that is *both* one- and two-photon-allowed. This suggests that further optimization of the molecular properties to enhance either A- or B-term scattering could yield molecules with significantly larger hyper-Raman cross sections.

In resonance Raman scattering, it is well-known that interference effects in the spectrum may arise when multiple excited states contribute to the scattering process. This typically requires spectral overlap between the excited states, as the Franck–Condon scattering intensity falls off rapidly with detuning from resonance. This is *not* the case, however, for B-term scattering, and our calculations showed significant interference between the two lowest excited states in the RHR spectra even though they are separated by more than 100 nm. On resonance with S_2 , we found that the constructive interference between the S_2 and S_1 states amounts to roughly 34% the intensity while the contributions from only S_2 or S_1 contribute 53 and 13%, respectively. While the interference is constructive when resonant with S_2 , we found it to be destructive when resonant with S_1 .

The interference is caused by a combination of the detuning from resonance and the relative orientations of the one- and two-photon transition moments and their derivatives on the two excited states. The interference from the detuning was found to cause constructive interference at S_1 and destructive interference at S_2 (see the SI). For the S_2 state, we found that the two-photon transition moment (S_{20}) and the nuclear dependence of the one-photon transition moment ($d\mu_{20}/dQ$) are almost antiparallel. However, for the S_1 state, the one-photon transition moment (μ_{10}) and the nuclear dependence of the two-photon transition moment (dS_{10}/dQ) are parallel. This leads to a change in the sign of the interference. Thus, the observed interference is a result of the combined effect of the interference from detuning and the sign arising from the transition moments.

This work has demonstrated that the complex interplay of electronic excited states encountered in RHR scattering is now accessible using first-principles theory for large molecules such as R6G. This agreement was achieved only after the inclusion of non-Condon terms in the calculations, which yields important insights into the two-photon properties of the molecular chromophore. Furthermore, this work suggests that non-Condon terms and interference effects are more important in determining two-photon properties than previously expected. Future studies utilizing RHR and SEHRS will elucidate the complex interplay of electronic excited states encountered in multiphoton processes such as all-optical switching, energy up-conversion, and biological imaging.

■ ASSOCIATED CONTENT

S **Supporting Information.** Details of the experiment and theory and complete ref 5. This material is available free of charge via the Internet at <http://pubs.acs.org>.

■ AUTHOR INFORMATION

Corresponding Author

jensen@chem.psu.edu; jcamden@utk.edu

■ ACKNOWLEDGMENT

This work was supported by the University of Tennessee, the UT/ORNL Joint Institute for Advanced Materials, and the U.S. Department of Energy, Office of Basic Energy Sciences, under Award DE-SC0004792. This work was also supported by Pennsylvania State University, the U.S. National Science Foundation under Grant CHE-0955689, and the Air Force Office of Scientific Research under Contract FA9550-10-C-0148.

■ REFERENCES

- (1) Hales, J. M.; Matichak, J.; Barlow, S.; Ohira, S.; Yesudas, K.; Brédas, J.-L.; Perry, J. W.; Marder, S. R. *Science* **2010**, *327*, 1485.
- (2) He, G. S.; Tan, L. S.; Zheng, Q.; Prasad, P. N. *Chem. Rev.* **2008**, *108*, 1245.
- (3) Pawlicki, M.; Collins, H. A.; Denning, R. G.; Anderson, H. L. *Angew. Chem., Int. Ed.* **2009**, *48*, 3244.
- (4) So, P. T. C.; Dong, C. Y.; Masters, B. R.; Berland, K. M. *Annu. Rev. Biomed. Eng.* **2000**, *2*, 399.
- (5) Cumpston, B. H.; et al. *Nature* **1999**, *398*, 51.
- (6) Kawata, S.; Kawata, Y. *Chem. Rev.* **2000**, *100*, 1777.
- (7) Larson, D. R.; Zipfel, W. R.; Williams, R. M.; Clark, S. W.; Bruchez, M. P.; Wise, F. W.; Webb, W. W. *Science* **2003**, *300*, 1434.
- (8) Milojevich, C. B.; Silverstein, D. W.; Jensen, L.; Camden, J. P. *ChemPhysChem* **2011**, *12*, 101.
- (9) Kelley, A. M. *Annu. Rev. Phys. Chem.* **2010**, *61*, 41.
- (10) Chung, Y. C.; Ziegler, L. D. *J. Chem. Phys.* **1988**, *88*, 7287.
- (11) Baranov, A. V.; Bobovich, Y. S. *JETP Lett.* **1982**, *35*, 181.
- (12) Golab, J. T.; Sprague, J. R.; Carron, K. T.; Schatz, G. C.; Van Duyne, R. P. *J. Chem. Phys.* **1988**, *88*, 7942.
- (13) Kneipp, K.; Kneipp, H.; Itzkan, I.; Dasari, R. R.; Feld, M. S. *Chem. Phys.* **1999**, *247*, 155.
- (14) Murphy, D. V.; Vonraben, K. U.; Chang, R. K.; Dorain, P. B. *Chem. Phys. Lett.* **1982**, *85*, 43.
- (15) Makarov, N. S.; Drobizhev, M.; Rebane, A. *Opt. Express* **2008**, *16*, 4029.